Quasielastic scattering: slow dynamics of glasses

H. Franz [a,*], W. Petry [a] and A.Q.R. Baron [b]

[a] *Physik Department E13, Technische Universität München, D-85748 Garching, Germany*
[b] *Spring-8 / JASRI, Hyogo 678-12, Japan*

The dynamics of glasses shows some distinct differences with respect to the crystalline state. Both in the short time regime (boson peak) and the microscopically slow regime (alpha- and beta-relaxation) there are glass-typical features. The outstanding sharpness of nuclear transitions offers a new tool to investigate the properties of glasses at long times, i.e., some nanoseconds to microseconds. The article will give a short introduction to glass-dynamic and convenient parameters for the theoretical description and will summarize recent results on model systems.

Keywords: quasielastic scattering, structural relaxation, non-resonant scattering, disordered systems

1. Introduction

Studying the dynamic properties of amorphous materials is an involved task. In a perfect crystalline solid, symmetry and long range order make things relatively simple: the structure is defined by few Fourier components, a well defined number of excitations (phonons) is sufficient to describe the thermal properties. Diffusion takes place via jumps to nearest or next-nearest neighbour lattice sites, or, in more complex systems, via interstitial sites. All this is different for an amorphous solid: an infinite number of Fourier components is needed to describe the structure, excitations are distributed over a broad energy range and the long range transport of atoms is still a topic of controversy [1,2].

Similar difficulties apply to the transition from a viscous liquid to a solid glass. While crystallization of a liquid is a structural transition from disorder to a periodic lattice, no significant structural change can be observed for the liquid–glass transition; the absence of long range order is maintained independent of whether the glass forming liquid is viscous or solid. What changes are the internal mobilities. Only few years ago a full atomistic theory, mode coupling theory MCT [3] has been proposed, describing the liquid–glass transition as a crossover from an ergodic (liquid) to a non-ergodic state (solid) on a microscopic scale. In its idealised version a unique transition temperature T_c is proposed: with increasing temperature localized mobility disintegrates to long range structural relaxation. In real glasses the concept of a

* Present address: DESY, HASYLAB, Notkestr. 85, D-22603 Hamburg, Germany.

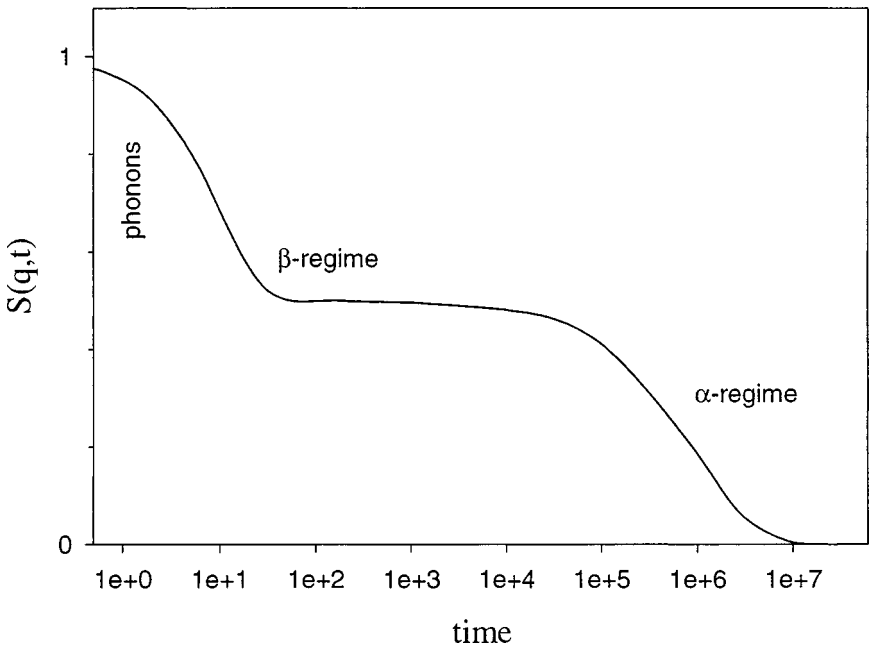

Figure 1. Schematic representation of the correlation function or intermediate scattering law of an amorphous solid.

liquid–glass transition as a breaking of ergodicity has to be refined. On long time scales ergodicity is always restored by additional transport processes like hopping or plastic flow. Consequently, the transition is smeared out, even in a simple system like the ionic glass former $Ca_{0.4}K_{0.6}(NO_3)_{1.4}$ (CKN). However, the concept of a dynamical liquid-to-glass transition is observed in its full beauty in colloidal suspensions as a macroscopic realization of the hard sphere model [4].

Typically, T_c lies some 20–50% above the caloric glass transition temperature T_g. The latter is defined, for example, by the excess specific heat observed in a differential scanning experiment. This increase in the specific heat reflects the onset of the structural relaxation in the time window given by the speed of the thermal ramp [5]. Therefore, T_g is not a unique transition temperature but depends on the time scale of the experiment [6].

The motion of an atom or molecule is most comfortably described in terms of the time dependent density–density correlation function $\Phi(t)$ (also called intermediate scattering function $S(q,t)$, see figure 1 [7]). To be strict we must discriminate between the self-correlation function $\Phi_s(t)$ and the so called pair-correlation function $\Phi(t)$. The first one describes the single particle dynamics as seen in incoherent scattering experiments, while the latter reflects the temporal evolution of correlations between all atoms or molecules. Nuclear resonant scattering methods give access to both correlation functions, as will be argued below. For simplicity we will discuss the properties of $\Phi(t)$ in this section and only mention the difference to $\Phi_s(t)$ where necessary.

In a glass three distinct regions of time may be discerned. At very short times – picoseconds or less – propagation of sound and thermal vibrations dominate. They give raise to the initial decay in the correlation function. Characteristic for glasses or more generally disordered systems is the so called boson peak, an excess excitation with respect to the crystalline counterpart at an energy usually near 4 meV. As this is in general a harmonic feature curves measured at different temperatures coincide after rescaling with the Bose–Einstein occupation factor [8]. Recent theoretical work attributes it to the structural disorder of a glass [9]. Adjacent to the phononic region the so called β-relaxation governs the correlation function. It is identified as a local rattling of the molecules in a cage formed by their neighbours. This cage effect confines the molecules to a limited region in space, so no long range transport takes place yet. Long range motion is reflected in the structural- or α-relaxation, the final decay of $\Phi(t)$ to zero. According to the Einstein–Smoluchovski equation this decay time τ is intimately connected to the diffusion coefficient

$$D = \frac{l}{6\tau}, \tag{1}$$

where l is a typical jump distance.

In contrast to transport in crystalline systems the final decay of $\Phi(t)$ in amorphous materials is well described by a Kohlrausch function [10]:

$$\Phi(t) = f_q \cdot \mathrm{e}^{-\{t/\tau_K\}^\beta} \tag{2}$$

with the stretching parameter $\beta < 1$. In the limit of large $q = 4\pi/\lambda \sin\theta$ (scattering angle 2θ), i.e., far beyond the structure factor maximum, this function was shown to coincide with the MCT relaxation function [11]. The amplitude of the structural relaxation, or the heights of the plateaux in $\Phi(t)$, is the Debye–Waller factor f_q. In general practice the stretching parameter β turns out to depend both on momentum transfer $\hbar q$ and temperature and is limited to an interval between 0.3 and 1. Over a wide range in temperature however, this dependence is very weak and the time–temperature-superposition principle holds; by a mere rescaling of the time axis and normalisation of the amplitude all relaxation functions fall on a common master curve [12,13]. The MCT glass transition is located where the structural (α-) relaxation decouples from the localised β-relaxation. Below T_c viscous transport is frozen in and, in an idealized theory, only localised motion remains. In the liquid region the relaxation time is proportional to the viscosity, as identified by Stokes and Einstein.

Although neutron scattering has produced a vast collection of data shining light on the atomistic interpretation of the glass transition, results concerning the structural relaxation are obtained only for temperatures above T_c, i.e., in the liquid state, as energy resolution is limited to some 10 neV. Inelastic light scattering is superior in energy resolution and has also produced data below T_c [14].

Near T_c, where relaxation times are of the order of 10 ns or more, nuclear resonant scattering (NRS) may contribute to a better understanding of the topic. Due to the sub-Ångstrom wavelength used in NRS it opens the window to study the relaxation

on a sub-atomic length scale. Most other techniques determine relaxation times either on a macroscopic length scale or at best down to intermolecular distances. NRS with its possibility for high momentum transfer yields data on a length scale down to 0.5 Å. First neutron scattering data [15] indicate that in this region (beyond the first maximum of the structure factor) the hydrodynamic scaling of the diffusion coefficient or relaxation time with q^{-2} no longer holds and new physics emerges.

In the following two sections we want to summarise the experiments done on glasses up to now as examples for the different techniques to measure quasielastic scattering: (1) resonant scattering from samples containing iron, (2) nonresonant or Rayleigh scattering from arbitrary samples. We will give only very few details on scattering theory that can be found in other sections of this issue and in [16,17]. Only equations used to explain the data will be given. Also experimental details will be kept rather short since there are chapters in this book dedicated to the relevant beamline equipment. Finally, we compare the results and prospects of quasielastic nuclear resonant scattering with competing and complementary techniques like quasielastic Mössbauer spectroscopy (QMS), quasielastic neutron scattering (QNS) and light scattering (LS).

2. Resonant scattering experiments

The most direct way to study atomic motions by NRS techniques is to look directly at the motion of ^{57}Fe nuclei (or another Mössbauer isotope) in the sample via coherent forward scattering and incoherent scattering into "4π". In this respect it is similar to QMS or other spectroscopic methods [18]. Any displacement during the emission of the γ-rays will give rise to a time dependent phase shift in the emitted wavelet (with respect to the static surroundings) and thus destroy the coherence in the forward channel. As current detectors offer only a limited time resolution, motions on short (picosecond) time scale may not be detected directly. Rather they give rise to the Lamb–Mössbauer factor f_{LM}. Motions in the time interval of the measurement may be observed by an accelerated decay with respect to the static case. This effect was predicted theoretically by Smirnov and Kohn [19] and shortly afterwards measured by Sepiol et al. [20] for a crystalline system, Fe_3Si. The case of an amorphous solid is much more involved. Firstly, f_{LM} is rather small in the temperature range where diffusion sets in on the time scale of the experiment (some 100 ns), so the signal is notoriously weak. Further, the time dependence of the forward scattered intensity may be obscured by two counter-balancing effects. With increasing temperature diffusion may enhance the decay with time. But increasing temperature also means a decreasing f_{LM}, thus a smaller effective thickness and a slower decay in the coherent channel. This problem may be solved by measuring both coherent forward scattering and incoherent scattering into finite scattering angles.

As the scattering process involves the absorption and reemission of photons, the momentum transfer is restricted to the momentum of the γ-quantum, i.e., 7.3 Å^{-1} for ^{57}Fe. Thus single particle dynamics is observed on an atomic to sub-atomic scale.

Macroscopic techniques measure integral properties of the dynamics and are known to yield results proportional to the relaxation times measured at the structure factor maximum, that is, on the length scale of the nearest neighbour distance. Further, they see the coherent dynamics, the pair-correlation. For two reasons results measured by nuclear resonant scattering may differ from those by rheology or dielectric spectroscopy, for example. NRS measures single particle correlation instead of pair-correlation and the length scale is smaller. This may result in different relaxation times τ at a given temperature and in a different temperature dependence $\tau(T)$. It is the challenge of NRS that it exploits a space–time region that is hardly accessible by other scattering methods.

The problem arises to find glass-forming systems containing iron. Though other isotopes have been used for nuclear resonant scattering [21], for the time being only ^{57}Fe is suitable to carry out quasielastic scattering experiments. Among the model systems used to study the glass properties, like glycerol, ortho-terphenyl, calcium-potassium-nitride or polymers [22], there is not a single one containing iron or an element which may be substituted by iron. So composite systems seem the only amenable path: a component containing iron (like FeCl or ferrocene $Fe(C_5H_5)_2$) is dissolved in a glass-forming system. This solution, however, may lead to problems concerning miscibility and in the interpretation of the dynamics measured in experiments: does the iron containing compound really reflect the overall dynamics described in theories of the amorphous state?

2.1. Experimental

For a first experiment a mixture of ferrocene and dibutylphthalate was chosen. It is a well-known glass-former and was already studied by Ruby et al. using QMS [23],

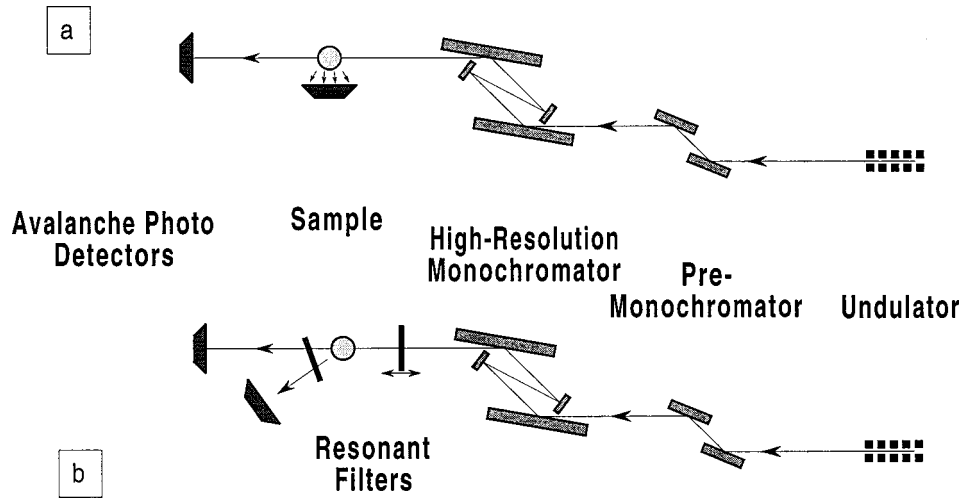

Figure 2. Set-up for (a) resonant and (b) nonresonant quasielastic scattering experiments at ID18, ESRF, Grenoble.

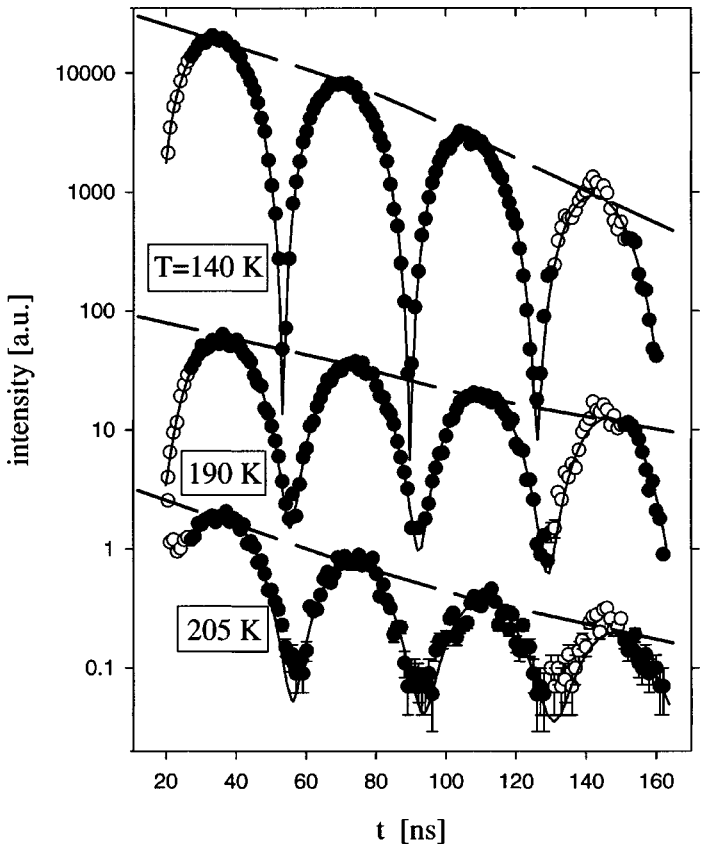

Figure 3. Nuclear resonant forward scattering from a sample of ferrocene/dibutylphthalate at different temperatures [16]. The structural relaxation is reflected in the accelerated decay of the intensity indicated by the dashed line. Note that the curvature of the experimental data changes from concave at low temperatures (thickness effect) to convex at higher temperatures (typical for stretched exponential functions).

by dielectric susceptibility [24] and several other techniques. For a ferrocene concentration of 4.4% the calorimetric glass transition temperature T_g was determined by differential scanning calorimetry (DSC) to 181.5 K.[1] The ferrocene $Fe(C_5H_5)_2$ was enriched to 95% in ^{57}Fe in order to optimise the signal. Figure 2(a) shows the set-up. Further details may be found in [16].

2.2. Results

Figure 3 shows the forward scattered intensity of the sample at various temperatures, starting well below the calorimetric glass-transition up to values some 30 K above. The simultaneously measured incoherent intensity shows a pure exponential

[1] We would like to stress that this value depends on the thermal history of the sample and the experimental conditions. It is not considered as a physical transition temperature.

decay and was not analysed any further. The value of the intensity extrapolated to $t = 0$, which is independent of f_{LM} [19], however, served as an important quantity to normalise the data. From a theoretical point of view, the intensity scattered into finite angles (mostly called "incoherent scattering", though it also contains contributions from coherent scattering) is also influenced by diffusion. But as the Lamb–Mössbauer factor is usually rather small at temperatures where diffusion sets in on the time scale of the Mössbauer resonance, the dominant part of incoherent scattering is scattering with recoil (called $I^B_{4\pi}$ in [19]) and thus is not sensitive to diffusion. This was confirmed by the structureless data we obtained in the detector set up at finite scattering angles.

The dominating feature of the forward time-spectra, the beating with frequency 27 MHz due to the quadrupole-splitting in ferrocene, was found to be almost constant in the whole temperature interval. We observe only a slight motional narrowing of 2.6% when increasing the temperature from 140 K to 205 K. The diffusion manifests itself in the accelerated decay of the envelope of the scattering curve (dashed line). This rate is presented in figure 4 as a function of temperature. At low temperatures it is determined by speed-up effects [25]: a decrease of the Lamb–Mössbauer factor with increasing temperature causes a decrease in effective thickness. For very thin samples the decay approaches the natural one. But instead of decreasing monotonically the curve bends up – starting at 185 K when diffusion sets in on a microsecond time scale and the decay is again accelerated. In contrast to this the scattering into finite angles

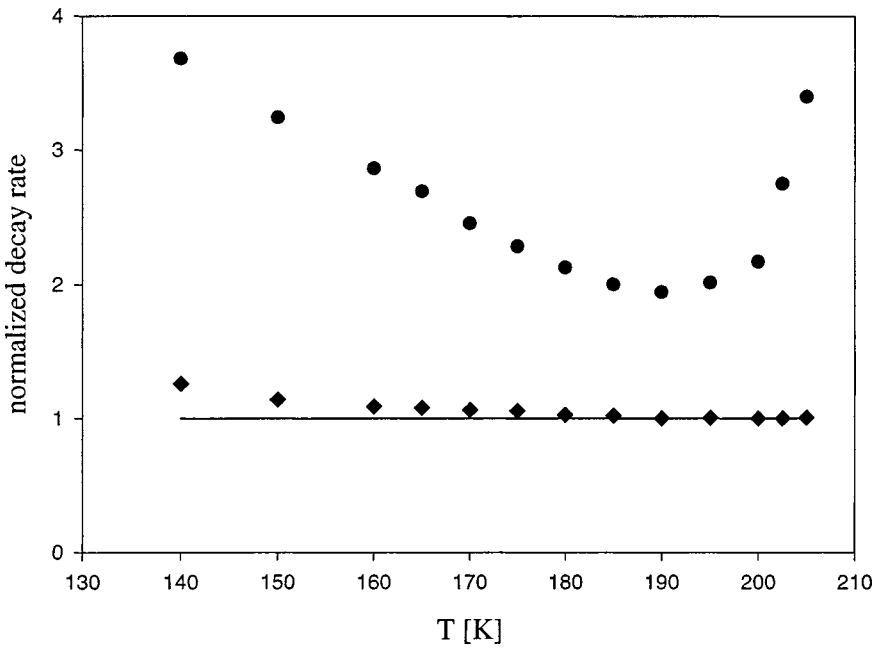

Figure 4. Effective decay rate of the forward scattered (circles) and 4π-scattered radiation from ferrocene/dibutylphthalate. The solid line indicates the natural decay with $T_{1/2} = 98$ ns.

shows a decay with the natural lifetime of 141 ns as it is dominated by scattering with recoil. Only at the lowest temperatures, where f_{LM} is of the order of 0.08, the small contribution of recoilless scattering speeds up the decay slightly.

The forward scattering was fitted using the theory as developed in [19]. A temperature dependent quadrupole splitting Ω and a Kohlrausch relaxation function (see above) was used. In contrast to simple exponential relaxation, prevailing in crystalline systems, the forward scattered intensity in this case may not be calculated analytically in reasonable approximation. So a Fourier transformation algorithm had to be applied [16]. The intensity as a function of time is given by

$$I(t) = I_0 \left| \int \frac{\mathrm{d}\omega}{2\pi} \cdot \mathrm{e}^{-\mathrm{i}\omega t} \left[\exp\left(-\frac{T_{\mathrm{eff}}}{2} \sum_{\pm} \frac{1}{2} \Phi_{\mathrm{s}} \left(\omega \pm \frac{\Omega}{2} \right) \right) - 1 \right] \right|^2, \tag{3}$$

where $\Phi_{\mathrm{s}}(\omega)$ is the Laplace transformation of the Kohlrausch relaxation function with $\beta = 0.5$ [26–28]. $T_{\mathrm{eff}} = 193$ is the effective thickness of the sample at $T = 0$ and I_0 the incident intensity as prepared by the high-resolution monochromator system. We stress that resonant scattering is testing the *self-correlation* function $\Phi_{\mathrm{s}}(t)$.

The most important parameter obtained by the fitting, the relaxation time τ_K, is presented in figure 5 as a function of temperature. The mean relaxation time $\langle \tau_K \rangle = \tau_K \beta^{-1} \Gamma(\beta^{-1})$ is shown, a value directly comparable for different relaxing quantities measured. For comparison we also plotted the mean relaxation times determined from

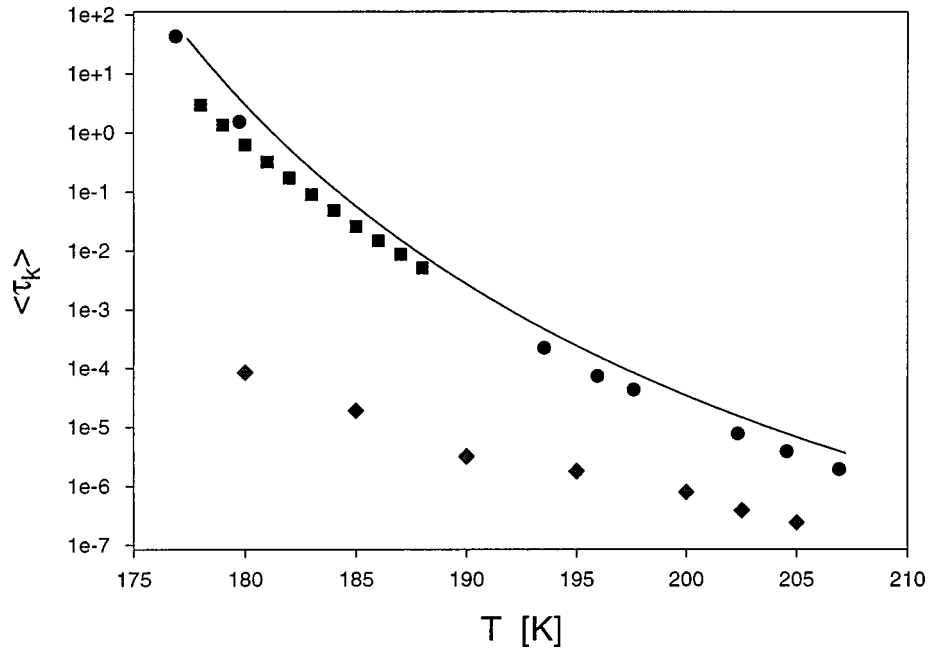

Figure 5. Kohlrausch relaxation times for ferrocene/dibutylphthalate. Solid line: viscosity data [27], circles: dielectric data [26], squares: dielectric data [27], diamonds: NRS [16].

viscosity and dielectric relaxation measurements [26,27]. Two features emerge from this data analysis:

(1) Relaxation times are approximately two orders of magnitude shorter compared to the dielectric measurements. This is easily explained by the small length scale (high q-value) on which motion is observed. In the hydrodynamic range the relaxation time is proportional to q^{-2} or even stronger for large q [15]. More striking is the fact that the temperature dependence does not coincide with that of the other experiments; the dependence is much weaker. Considering figure 1 we immediately realise that there is a lower limit of relaxation times given by the initial decay in $\Phi(t)$ caused by phonon excitations. Extrapolating the value measured at the lowest temperature $T = 180$ K, using the temperature dependence of viscosity we would arrive at a value for $\langle \tau_K \rangle$ close to a few picoseconds in the liquid regime. But the structural relaxation time may not be faster than typical vibration times, which are of the same order of magnitude. Therefore, the temperature dependence has to be the weaker, the shorter the length scale.

(2) The second parameter extracted from the fit is the Lamb–Mössbauer factor shown in figure 6. At low temperatures it decays exponentially, the ferrocene–dibutylphthalate behaves rather harmonically, similarly to many other glasses. Starting at 175 K (some 10 K below the measured T_g) we find deviations from this trend. We interpret this as an indication of β-relaxation, though any anharmonic motion would manifest itself in this way.

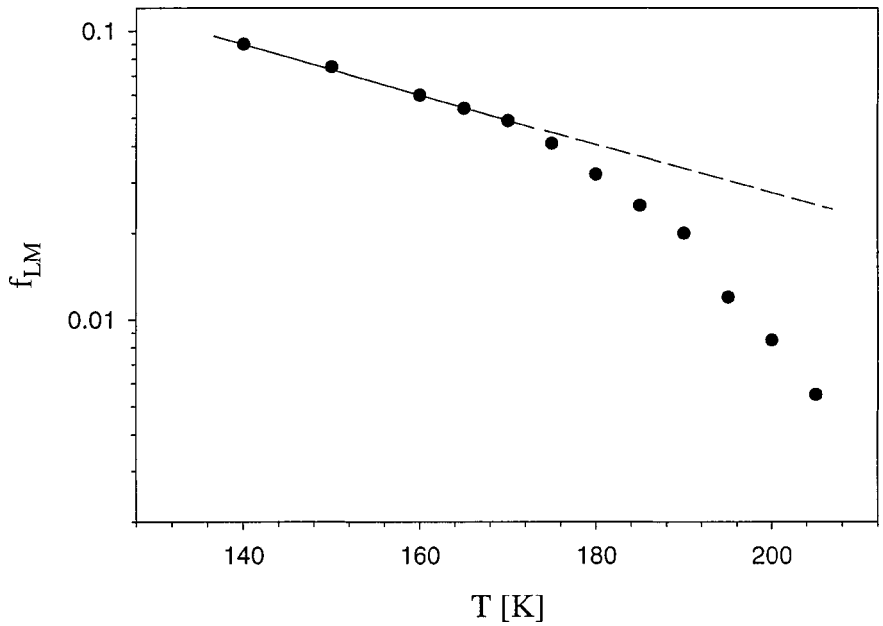

Figure 6. Lamb–Mössbauer factor of ferrocene/dibutylphthalate. Note the deviation from a harmonic (straight line) decay starting near 170 K.

To conclude, we want to stress that although NFS works in the same $q-\omega$ range as QMS the fact that intensity is observed directly as a function of time facilitates the detection of very small quasielastic broadening (long relaxation times). This is caused by the fact that NFS measures only the resonant intensity, other contributions being gated out electronically. QMS detects the resonant effect relative to a background, this always requires far better statistics. This is the main reason for shorter integration times. The detection of tiny relaxation effects is greatly facilitated by the absence of an analyser and the convolution of the signal with the respective resolution function.

3. Nonresonant scattering experiments

The measurements of resonant scattering described above have two drawbacks when compared to general scattering methods: (i) the momentum transfer is fixed by the wave vector of the Mössbauer transition involved, and (ii) we need a Mössbauer isotope in the sample, but most physical problems cannot be studied in samples containing iron (up to now the only feasible isotope for this kind of measurement). So we started to investigate possibilities to perform quasielastic scattering experiments using arbitrary samples (nonresonant scattering). The idea was to translate the Rayleigh Scattering of Mössbauer Radiation (RSMR) technique [29] to the time regime using synchrotron radiation. This allows one to arbitrarily choose the momentum transfer by changing the scattering angle and thus also study the length scale of the excitation. Nuclear resonance scattering now serves as a tool to first monochromatise the incident radiation and second, after scattering from the sample, to analyse the energy transfer before detection. The general layout of the experiment is thus equivalent to the well-known triple-axis geometry.

3.1. Experimental

The set-up used for this kind of experiments is shown in figure 2(b). As monochromator and analyser stainless steel foils (95% enrichment, $T_{\mathrm{eff}} = 27$) have been used. The respective resonance energies have been shifted relative to each other using a Mössbauer drive in constant velocity mode. The detector and analyser may be placed at any scattering angle 2θ in order to scan the q dependence of the scattering. In the case of *elastic* scattering the two resonant waves emerging from analyser and monochromator interfere to give an intensity pattern similar to the time spectrum of ferrocene (compare lowest curve in figure 7 with figure 3). For ferrocene the modulation is caused by a quadrupole splitting, whereas in this case it is due to the beating of two very monchromatic and coherent waves with slightly different energies. Further, as the stainless steel foils are rather thick, a dynamical beating is overlaying this cosine modulation. An inelastic scattering process in the sample now adds a time dependent phase to the scattered waves. Quasielastic scattering means a distribution of these phase shifts and consequently the interference with the reference wave from the analyser will be disturbed.

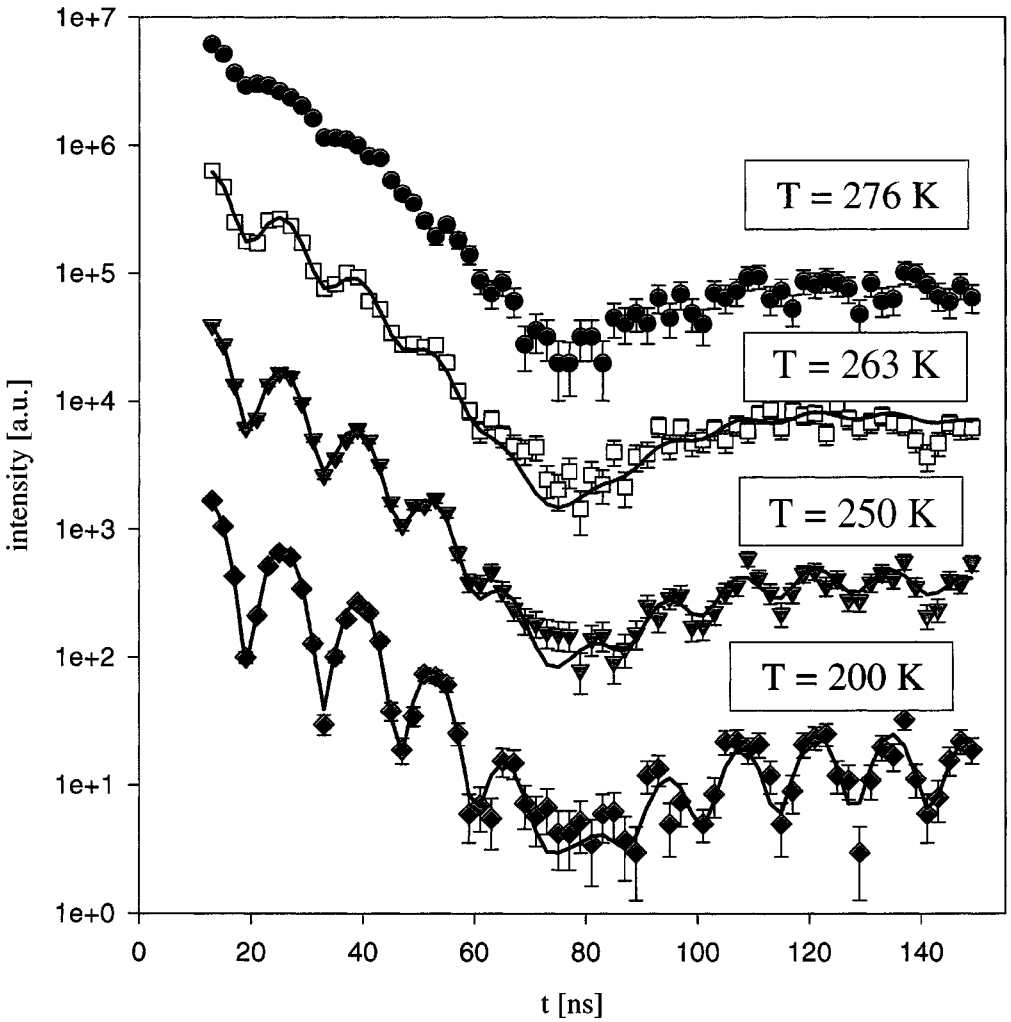

Figure 7. Time-domain interference patterns from glycerol measured at the structure factor maximum as a function of temperature. With increasing temperature the oscillations are damped out.

As the aim of this first experiment [17] was to demonstrate the feasibility of this kind of technique, we chose glycerol, a well investigated glass-forming system, for our experiments. We first studied the temperature dependence of the quasielastic scattering at the maximum of the structure factor ($q = 1.5$ Å^{-1}). In a second step, we changed the scattering angle to determine the q-dependence of the relaxation. As the data is not yet complete, these results will be discussed elsewhere.

3.2. Results

Figure 7 shows the intensity pattern measured at the first maximum of the structure factor for different temperatures. At the lowest temperature (200 K) the scattering

is mainly elastic, structural relaxation happens in the ms region far beyond our time window. Only phonon excitations cause a constant damping of the modulation. When increasing the temperature two effects occur: (1) the Debye–Waller factor is increased and thus the amplitude of the cosine oscillation is decreased, and (2) the relaxation time approaches the time window of the experiment. This means that a substantial fraction of the atoms move while the sample is illuminated by the coherent resonant radiation emerging from the monochromator, resulting in a time dependent, random phase shift of the waveletts. When combined with the reference wave from the analyser (the delayed scattered radiation is transmitted through the analyser with only negligible nuclear absorption, as the two resonances are separated) the phase shift is reflected in a loss of coherence and thus a time dependent damping of the oscillations. This is demonstrated in figure 7. With increasing temperature the fading of the oscillations is progressively shifted to shorter times.

Writing down the scattering amplitudes in Born approximation we arrived at the following equations for the scattered amplitude [17]:

$$E(q,t) \propto G(t) \cdot \mathrm{e}^{-\mathrm{i}(\omega_0-\Omega)t} \sum_n \mathrm{e}^{\mathrm{i}qr_n(t)} + G(t) \cdot \mathrm{e}^{-\mathrm{i}\omega_0 t} \cdot \sum_n \mathrm{e}^{\mathrm{i}qr_n^0} \tag{4}$$

and, after multiplication with the complex conjugate, for the intensity:

$$I(q,t) \propto \left|G(t)\right|^2 \left[S(q) + \cos(\omega t) S(q,t)\right]. \tag{5}$$

$G(t)$ describes the response of the monochromator and analyser foils (assumed to be identical), ω_0 is their resonance energy and Ω the shift induced by the Mössbauer drive. r_n^0 denotes the position of atom n at the time when the sample is hit by the synchrotron radiation pulse ($t = 0$) and $r_n(t)$ is the subsequent evolution of the position. $S(q)$ and $S(q,t)$ indicate the static structure factor and intermediate scattering function, respectively. The first term in (4) is the scattered resonant radiation from the first foil, while the second describes the reference wave from the analyser. In contrast to resonant scattering this experiment studies the *pair-correlation* function $\Phi(t)$.

Using again a Kohlrausch relaxation function with $\beta = 0.7$ taken from [13], we arrive at the relaxation times plotted in figure 8. For comparison data measured by neutron spin-echo [13] at the structure factor maximum and the viscosity of glycerol [30–32] divided by temperature are also included. While the neutron data in the liquid regime exhibit the same temperature dependence as the viscosity data, the synchrotron data measured at lower temperatures, approaching the amorphous state, show an increasing deviation from this trend. This fact was already observed using NMR [33], neutron spin-echo measurements [34] or molecular dynamics simulations [35].

4. Critical assessment and outlook

We have demonstrated in two examples the possibilities to investigate structural relaxation in glasses using quasielastic scattering of synchrotron radiation. New results

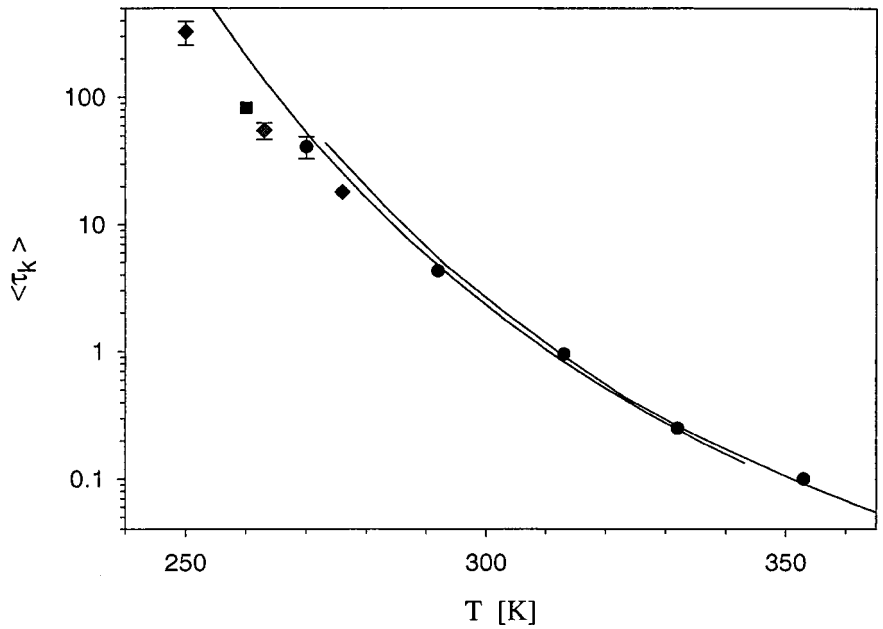

Figure 8. Kohlrausch relaxation times for glycerol. Solid line: viscosity data [30–32], circles: neutron spin-echo data [13], diamonds: NRS [17].

emerged from the improved energy resolution or, in other words, the extended time range accessible. We observed a deviation of the relaxation times from the simple scaling behaviour with viscosity on an atomic scale approaching the glass-transition. On larger scales (μm) [33] and in polymers [34] this effect has been known.

In the following we want to compare NRS to competing methods used to study the glass dynamics. We restrict ourselves to scattering methods although we are aware that other techniques like NMR, dielectric spectroscopy or mechanical probes have also made important contributions to the field.

The work-horse for studying microscopic dynamics is inelastic scattering of neutrons. It is unique in observing the short time dynamics of any solid or liquid. It is a more involved task to get access to the relaxational dynamics which occurs on longer time scales. Using spin-echo techniques the time window may be extended to some 100 ns, but at the expense of atomic resolution in space (up to now this high resolution is only achieved at low scattering vector q). The better resolution of nuclear resonant techniques and its complementary q-range now extends the time–space window to detect relaxations and diffusion in solids, in particular in glasses near the transition temperature T_c.

Light scattering is of course superior regarding the resolution in energy, respectively the time window of the measurement. Using photon-correlation spectroscopy even relaxations on a time scale of minutes are accessible. Its drawback is the long wavelength and accordingly limited spatial resolution. But in the hydrodynamic range precious results have been obtained in the last years [36].

A severe drawback of NRS, in particular when dealing with stretched exponential relaxations typical for disordered systems, is the limited time window where data may be taken. In the standard operation mode of third generation synchrotrons some 10 ns to 200 ns, i.e., 1.3 orders of magnitude, may be used. This currently limits the possibilities to study the functional dependence of $\Phi(t)$. So up to now only the combination with data from neutron scattering or similar methods allows the determination of the shape of $\Phi(t)$, i.e., to separate exponential decay from stretched exponential decay. If single bunch mode would be available on 3rd generation machines in sufficient quantity, an extension of the time window to some 2.5 orders of magnitude may be realistic, however at the expense of intensity. Neutron or light scattering can cover some 3.5 orders of magnitude with a single instrument; when different spectrometers are combined this may be extended even further.

A certainly very promising prospect is the combination of coherent neutron scattering (spin-echo) and nonresonant quasielastic scattering of synchrotron radiation. As both techniques measure the relaxation of density fluctuations in a complementary and partly overlapping q-range, results may be directly combined (notwithstanding corrections for different scattering cross sections). The different scattering cross sections may even be used to perform contrast variation experiments, and in this way yield more valuable information. In principle results obtained by resonant scattering could be combined with incoherent neutron scattering. But iron has a negligible incoherent scattering cross section for neutrons and the maximum momentum transfers q obtainable by high resolution INS is far below the value of 7.3 Å^{-1} dictated by the nuclear resonance.

Acknowledgement

The authors are grateful for the support by the nuclear resonance group at ESRF and to U. van Bürck and G. Smirnov for helpful discussions.

References

[1] *Proceedings of the 3rd Discussion Meeting on Relaxations in Complex Systems*, Vigo; to be published in J. Non-Cryst. Sol. (1998).
[2] H. Ehmler, A. Heesemann, K. Rätzke and F. Faupel, Phys. Rev. Lett. 80 (1998) 4919.
[3] W. Götze and L. Sjörgren, Rep. Prog. Phys. 55 (1992) 241.
[4] W. van Megen and S.M. Underwood, Phys. Rev. E 49 (1994) 4206.
[5] R. Brüning and K. Samwer, Phys. Rev. B 46 (1992) 11318.
[6] W. Götze, in: *Liquids, Freezing and the Glass Transition* (Les Houches), eds. J.P. Hansen, D. Levesque and D. Zinn-Justin (North-Holland, Amsterdam, 1991).
[7] L. van Hove, Phys. Rev. 95 (1954) 249.
[8] J. Wuttke, J. Hernandez, G. Li, G. Coddens, H.Z. Cummins, F. Fujara, W. Petry and H. Sillescu, Phys. Rev. Lett. 72 (1994) 3052.
[9] W. Schirmacher, G. Diezemann and C. Ganter, Phys. Rev. Lett. 81 (1998) 136.
[10] R. Kohlrausch, Ann. Phys. (Leipzig) 91 (1854) 56 and 179.

[11] M. Fuchs, J. Non-Cryst. Sol. 172–174 (1994) 241.
[12] F. Mezei, W. Knaak and B. Farago, Phys. Rev. Lett. 58 (1987) 571.
[13] W. Petry, E. Bartsch, F. Fujara, M. Kiebel, H. Sillescu and B. Farago, Z. Phys. B 83 (1991) 175.
[14] H.Z. Cummins, W.M. Du, M. Fuchs, W. Götze, S. Hildebrandt, A. Latz, G. Li and N.J. Tao, Phys. Rev. E 47 (1993) 4223.
[15] J. Wuttke, I. Chang, O.G. Randl, F. Fujara and W. Petry, Phys. Rev. E 54 (1996) 5364.
[16] A. Meyer, H. Franz, J. Wuttke, W. Petry, N. Wiele, R. Rüffer and C. Hübsch, Z. Phys. B 103 (1997) 479.
[17] A.Q.R. Baron, H. Franz, A. Meyer, R. Rüffer, A.I. Chumakov, E. Burkel and W. Petry, Phys. Rev. Lett. 79 (1997) 2823.
[18] W. Petry and G. Vogl, Materials Science Forum 15–18 (1988) 323.
[19] G.V. Smirnov and V.G. Kohn, Phys. Rev. B 52 (1995) 3356.
[20] B. Sepiol, A. Meyer, G. Vogl, R. Rüffer, A.I. Chumakov and A.Q.R. Baron, Phys. Rev. Lett. 76 (1996) 3220.
[21] O. Leupold et al., this issue, section IV-2.7.
[22] W. Petry and J. Wuttke, Transp. Theory Statist. Phys. 24 (1995) 1075.
[23] S.L. Ruby, B.J. Zabransky and P.A. Flinn, J. Phys. C6 37 (1979) 745.
[24] P.K. Dixon, L. Wu, S.R. Nagel, B.D. Williams and J.P. Carini, Phys. Rev. Lett. 65 (1990) 1108.
[25] G.V. Smirnov, Hyp. Interact. 97/98 (1997) 551.
[26] J. Dufour, L. Jorat, A. Bondeau, A. Sibilini and G. Noyel, J. Mol. Liq. 62 (1994) 75.
[27] N. Menon, S.R. Nagel and D.C. Venerus, Phys. Rev. Lett. 73 (1994) 963.
[28] M. Paluch, J. Ziolo, S.J. Rzoska and P. Habdas, Phys. Rev. E 54 (1996) 4008.
[29] D.C. Champeney, Rep. Prog. Phys. 42 (1979) 1017.
[30] V. Vand, Research 1 (1947) 44.
[31] J.B. Segur and A.E. Oberstar, Ind. Eng. Chem. 43 (1951) 2117.
[32] R. Piccirelli and T. Litovitz, J. Acoust. Soc. Am. 29 (1957) 1009.
[33] F. Fujara, B. Geil, H. Sillescu and G. Fleischer, Z. Phys. B 88 (1992) 195.
[34] D. Richter, R. Zorn, B. Farago, B. Frick and L.J. Fetters, Phys. Rev. Lett. 68 (1992) 71.
[35] W. Kob, Private communication (1998).
[36] G. Li, H.E. King Jr., W.F. Oliver, C.A. Herbst and H.Z. Cummins, Phys. Rev. Lett. 74 (1995) 2280.